Microhydrodynamic Analysis of Nanogrinding in Stirred Media Mills

D. Eskin, O. Zhupanska, R. Hamey, B. Moudgil, and B. Scarlett
Particle Engineering Research Center, University of Florida, Gainesville, FL 32611

DOI 10.1002/aic.10392
Published online March 23, 2005 in Wiley InterScience (www.interscience.wiley.com).

The dynamics of the milling media in a turbulent flow is considered. The mean velocity of the milling beads is calculated on the assumption that the power spent on stirring is transferred into the energy of turbulent eddies. The energy spent on stirring dissipates as a result of media–liquid viscous friction, lubrication, and by inelastic collisions of the beads with each other. The maximum force at which the milling beads can compress particles between them is calculated by the Hertzian theory of elastic impact. The frequency of compressions for a single particle is evaluated by probabilistic analysis. A criterion of milling efficiency, based on calculating the energy spent on the plastic particle deformation, is proposed. A numerical study of the milling bead dynamics and their interactions with the particles in the mixing tank is performed. The numerical results are in qualitative agreement with the experimental data. Both the numerical and experimental analyses show that, from the perspective of hydrodynamics, an optimization of stirred media mills can be achieved by choosing the optimum size and concentration of the milling media. © 2005 American Institute of Chemical Engineers *AIChE J,* 51: 1346–1358, 2005
Keywords: grinding, mixing, multiphase flow, simulation, slurries, turbulence

Introduction

The production of nanoparticles is of great importance to the developing nanotechnology industry. Usually, grinding is not the major method used for the production of nanoparticles because the particle strength increases rapidly with a decrease in particle size. Therefore fragmentation of nanoparticles is a very energy consuming process. The precipitation of nanocrystals from solution is currently a more widely used technology. However, in many cases grinding is the only method available for the production of nanoparticles of certain materials. For example, producing nanoparticles of many organic materials is possible only by mechanical size reduction, that is, grinding.

There are several types of mills that may be used for nanogrinding, such as planetary mills that are often used for mechanical alloying. In this case the milling balls move with high velocities and accelerations, which provide very high stresses and loading frequencies in the solids, leading to efficient particle fragmentation. One of the major disadvantages of planetary mills is a high vibration that decreases mill reliability and makes scaling-up of equipment difficult. The well-known grinding by cavitation can produce nanoparticles, although this method requires very high operational pressures. Moreover, the milling chamber lining in this case should be manufactured from expensive wear-proof materials such as diamonds. Another technique that can be successfully applied for nanogrinding is cryogenic milling. Most materials become brittle under conditions of low temperature that make particle fragmentation much easier. However, because the cryogenic grinding is relatively expensive its industrial applications are restricted.

The stirred media mill is a grinder that holds the greatest promise for producing nanoparticles in large quantities. Basically, this mill consists of a stirrer placed in the center of a fixed milling cylinder. Such a milling chamber is filled with a milling media (normally, spherical glass, steel, or ceramic beads) and a suspension that is a mixture of liquid (usually, water) and the product particles. As a result of stirring the suspension inside the mill is fluidized and generates intensive collisional motion

Correspondence concerning this article should be addressed to D. Eskin at deskin@erc.ufl.edu.

of milling beads with each other. The particles to be ground are trapped between the colliding beads, which leads to solids fragmentation.

During the past 15–20 years, many researchers have studied the stirred media milling both experimentally and theoretically. Usually, analysis of the stirred media mill performance was carried out through the use of a simple approach based on the dimensional criteria of *stress number* (SN) and *stress intensity* (SI) (see, for example, Kwade,[1] Kwade and Schwedes,[2] and Jankovic[3]). The SI is proportional to the kinetic energy of a milling bead in a centrifugal field. The SN, which is supposed to be proportional to the number of compressions of a single particle between two milling beads, is calculated on the basis of operating assumptions.

The dynamics of the milling media have also been previously studied, although these investigations were limited to dilute flows. Blecher et al.[4] carried out computations for laminar flow and Theuerkauf and Schwedes[5] for turbulent flow. Multiple trajectories of separate milling beads were computed and measured by Theuerkauf and Schwedes.[5] The need is to further develop a comprehensive theory describing the dynamics of the milling media and their interactions with the particles in the dense slurry flow.

Herein a model is proposed to describe the media dynamics based on the transformation of the kinetic energy of turbulence into the kinetic energy of the milling bead fluctuations. This model is used to study the beads–particles interactions. Assuming that the deformation of nanoparticles is plastic, an approach is proposed for estimating the total energy spent on deformation of the solids, which is used for comparative estimations of the grinding efficiency.

Note that grinding to nanosizes is possible only with the use of surfactants or other stability-enhancing techniques, which prevent particle agglomeration and decrease the particle surface energy (Rebinder effect; see, for example, Khodakov[6]) expediting solids fragmentation. This important aspect of nanogrinding is beyond the scope of the present paper.

Preliminary Estimates of the Flow Behavior in a Stirred Media Mill

We will consider a three-phase flow consisting of liquid (usually water), milling beads, and particles of the material to be ground. Because the primary interest is superfine and nanogrinding, our consideration is limited to the systems where the particles are much smaller than the milling beads.

There are different regimes of stirred media milling. The milling beads may be uniformly dispersed over a milling chamber if the intensity of turbulent dispersion is high enough to overcome radial stratification, which is caused by the centrifugal force. Alternatively, the flow may be stratified if the centrifugal acceleration predominates. If the bead density is much larger than that of the liquid medium and if the beads are large enough they can be strongly stratified, forming a moving bed around the chamber wall. In this case grinding is, to a great extent, caused by the shear between layers of the bed. In this regime the grinding mechanism is similar to that which can be obtained in a ball mill operating with a high rotation speed and it does not seem to be efficient. We thus limit this analysis to the regime of dispersed flow only. By our estimates this regime exists when the milling media are $<$200–300 μm and the rotation speed is several thousand rpm. Then, the flow is characterized by the developed turbulence. The energy transformation in a turbulent flow is the key to understanding the grinding mechanism. It is known that in a developed turbulent flow almost all of the power spent on liquid mixing transforms into kinetic energy of turbulent fluctuations[7] because the turbulent viscosity is much greater than the laminar viscosity. Many researchers successfully use the Kolmogoroff model of isotropic turbulence (see, for example, Landau and Lifshitz[7] and Levich[8]) to simulate processes in various mixing devices such as chemical reactors and crystallizers. According to this model, the turbulence structure is represented as a spectrum of eddies of varying size. The large eddies gradually transform into smaller ones at a constant rate of energy dissipation until they are reduced to the smallest size, λ_0, which is called the inner turbulence scale[7,8]

$$\lambda_0 = \left(\frac{\rho_m \nu_m^3}{\varepsilon_{tot}}\right)^{1/4} \tag{1}$$

where ν_m is the kinematic viscosity of the slurry that can be calculated by some empirical correlation (for example, Shook and Roco[9] and Nagata[10]), ρ_m is the slurry density, and ε_{tot} is the total dissipation energy rate per unit volume, which is equal to the turbulent dissipation energy rate in the case of developed turbulence.

According to Kolmogoroff, eddies smaller than λ_0 cannot exist because in a pure liquid their kinetic energy is transformed into heat as a result of viscous dissipation. Simple analysis shows that the theoretical inner turbulence scale for a dense slurry flow in a stirred media mill has a size of several microns. It can be easily shown that the Kolmogoroff mechanism of turbulent energy dissipation on a microscale in dense slurry flows is impossible.

The mean clearance between the milling beads can be calculated by[9]

$$\delta = \left[\left(\frac{c_{lim}}{c}\right)^{1/3} - 1\right] d_b \tag{2}$$

where c_{lim} is the limiting (packing) volumetric concentration of the beads and d_b is the bead size.

The limiting concentration for spherical particles is usually estimated to be equal to $c_{lim} \approx 0.6$.[9] It follows from Eq. 2 that, for example, if $\delta < 0.5 d_s$ the corresponding volumetric concentration c $>$ 18%. The distance δ is close to the mean free path of chaotically moving particles. Thus, even in relatively dilute slurries, the beads have fairly restricted freedom of motion with respect to each other. It seems that the flow of liquid between particles cannot be turbulent in such a dense medium. The volumetric concentration of the milling beads is usually high ($c > 0.2$–0.3). This paper considers slurries composed of beads that range in size from tens to hundreds of micrometers. Thus, it is clear that the energy of the turbulent fluctuations in a stirred media mill cannot be dissipated by the Kolmogoroff mechanism.

It is known (for example, Wylie et al.[11]) that in dense slurries the turbulent energy is transformed into kinetic energy of particles (the beads in this case) colliding with each other, and

into the kinetic energy of small volumes of liquid (added mass) surrounding these oscillating particles. The only available energy dissipation mechanisms in the slurry considered are: this oscillating energy dissipates through viscous media–liquid friction, the squeezing of liquid films between approaching beads (lubrication), and also through partially inelastic collisions of the beads with each other (see, for example, Wylie et al.[11] and Eskin et al.[12]).

It should be noted that—if the beads were absolutely smooth and no flow disturbances occurred—theoretically, the kinetic energies of approaching beads would not be sufficient to squeeze the liquid films between them and collisions would never occur. However, at high bead Reynolds numbers (in the motion relative to the liquid) the liquid film breaks down because of surface roughness of the beads or noncontinuum fluid behavior.[13] According to Sangani et al.[13] the dependency of the viscous dissipation on the nature of this breakdown is weak. Our estimates show that the Reynolds number of the beads in stirred media mills is relatively high. Wylie et al.[11] reported that the Reynolds number is high from the perspective of the influence of inertia effects on flow dynamics if it is larger than unity (in stirred media mill it can reach about 100).

Model of Turbulence Energy Dissipation at the Microscale

Although the flow in the milling chamber is very complicated it is sufficient for an approximate analysis to assume uniformly distributed dissipation energy rate.

In a stirred media mill the power applied to the stirrer P_w dissipates through fluctuating motions at the microscale. The total energy dissipation rate in this case consists of two components

$$P_w = \varepsilon_{tot} = \varepsilon_{visc} + \varepsilon_{coll} \tag{3}$$

where ε_{visc} is the energy dissipation rate arising from both the liquid–beads viscous friction and lubrication and ε_{coll} is the energy dissipation rate resulting from partially inelastic bead–bead collisions.

It is clear that the beads in an agitated slurry should have a nonuniform distribution of fluctuation velocities. To characterize the distribution, Wylie et al.[11] proposed a criterion W, calculated as the ratio of the particle relaxation time to the mean time of the bead free motion between collisions. If this criterion is much larger than unity, then the particle velocity changes slightly during the free path and an approximation to a Maxwellian gas is valid for nearly elastic particles. Assuming a Maxwellian velocity distribution W has the following form[11]

$$W = 24\sqrt{\frac{3}{\pi}}\, c g_0 \frac{m_b \Theta}{F d_b} \tag{4}$$

where F is the average drag force acting on a single bead; m_b is the bead mass; $\Theta = \langle v_b^2 \rangle/3$ is the granular temperature; $\langle v_b^2 \rangle$ is the bead–liquid relative mean-square velocity; and g_0 is the radial distribution function, taking into account the influence of beads volumes on the collision process. This function can be calculated by[14]:

$$g_0 = \frac{1 - 0.5c}{(1-c)^3} \tag{5}$$

Wylie et al.[11] reported that $W \geq 2$ is a satisfactory condition to assume Maxwellian distribution.

Estimates from the model of slurry microhydrodynamics presented herein show that in a stirred media mill the criterion W can be both higher and lower than unity. Note, that for the stirred media mill analysis, we do not require exact values but reliable estimate velocities and frequencies of the bead oscillations that are dependent on the stirring conditions. The condition $W \geq 2$ is not critical for the present study. Our analysis is based on the average fluctuation velocities of the beads. In the model of microhydrodynamics described below the fluctuation velocity distribution reveals itself only through the ratio of the mean relative bead–bead root-mean-square (rms) velocity to the mean relative bead–bead velocity. For Maxwellian distribution of the fluctuation velocities this ratio is $\sqrt{3\pi/8} = 1.085$.[15] Drazer et al.[16] and Marchioro and Acrivos[17] investigated the mechanics of particle fluctuations in homogeneous suspensions under conditions of slow shear using Stokesian dynamics. Reynolds numbers of particles were vanishingly small in this study. The simulations showed that, even at zero particle Reynolds numbers, the distributions of particle fluctuation velocities were Maxwellian if the solids concentration was relatively high (25% according to Marchioro and Acrivos[17]).

Thus, the Maxwellian distribution can take place even if the criterion W approaches zero. The calculations of Drazer et al.[16] showed that decreasing the solids concentration at vanishingly small Reynolds numbers leads to the transformation of Maxwellian velocity distribution to an exponential one. However, in the case of the exponential velocity distribution the ratio between the rms velocity and mean velocity is $\sqrt{12}/3 = 1.155$.[15] This ratio is only 6.5% higher than that for the Maxwellian distribution and thus the model of hydrodynamics can reliably be used for engineering calculations, even in the case of an exponential distribution. Another cause of a possible failure of the model of hydrodynamics could theoretically be the cluster formation at $W < 2$ discovered by Wylie and Koch[18] in their simulations by the multipole technique. However, the formation of clusters consisting of milling media is prevented by turbulence because the inner turbulence scale in a stirred media mill is usually significantly smaller than media size.

Thus, we will assume that the velocity distribution is Maxwellian and work with the average bead velocities using the theoretical coefficients known for this distribution.

The dissipation energy rate per unit volume, attributed to both viscous friction and lubrication, is determined as[11]

$$\varepsilon_{vis} = F\sqrt{3\Theta}\, n_b = 9\pi\mu_L d_b n_b \Theta R_{diss} \tag{6}$$

where $n_b = 6c/\pi d_b^3$ is the bead numerical concentration (number per unit volume) and R_{diss} is the dissipation coefficient that can be interpreted as an effective drag coefficient of the bead.

Wylie et al.[11] proposed calculating the dissipation coefficient R_{diss} as a linear superposition of the coefficient R_{diss0}, which takes into account the energy dissipation by squeezing the liquid film, and the term $\mathrm{Re}_\Theta K(c)$, which accounts for the dissipation arising from the bead–liquid viscous friction:

$$R_{diss} = R_{diss0} + \mathrm{Re}_\Theta K(c) \tag{7}$$

where Re_Θ is the bead Reynolds number based on the granular temperature ($\mathrm{Re}_\Theta = d_b\rho_L\Theta^{1/2}/\mu_L$), μ_L is the liquid dynamic viscosity, R_{diss0} is the dissipation coefficient for the case when relative motion of the bead–liquid is absent ($\mathrm{Re}_\Theta = 0$), and $K(c)$ is a coefficient.

The dissipation coefficient at zero particles–liquid slip R_{diss0} was calculated by Sangani et al.,[13] who used a modified multiple method for simulation of Stokes flow in a liquid and obtained the following correlation

$$R_{diss0} = k_1(c) - k_2(c)\ln \varepsilon_m \tag{8}$$

where

$$k_1(c) = 1 + 3\sqrt{\frac{c}{2}} + \frac{135}{64}c\ln c + 11.26c(1 - 5.1c + 16.57c^2 - 21.77c^3) \tag{9}$$

$$k_2(c) = cg_0 \tag{10}$$

and ε_m is the nondimensional bead–bead gap thickness at which the lubrication force stops continually increasing and becomes constant.

At the nondimensional gap ε_m, the liquid film breakdown occurs. According to Sangani et al.,[13] ε_m can be chosen equal to 0.003. Using the Lattice–Boltzmann method, Wylie et al.[11] computed suspension flows at various energy dissipation rates and solids concentrations. On the basis of the numerical results they obtained the following empirical correlation for $K(c)$

$$K(c) = \frac{0.096 + 0.142c^{0.212}}{(1 - c)^{4.454}} \tag{11}$$

The energy dissipation rate attributed to partially inelastic bead–bead collisions is calculated as[19]

$$\varepsilon_{coll} = \frac{12}{d_b\sqrt{\pi}}(1 - k^2)c^2\rho_b g_0\Theta^{3/2} \tag{12}$$

where k is the restitution coefficient for particle–particle collisions.

The calculations obtained from the model presented show that for a stirred media mill, the dissipation rate attributed to bead–bead collisions is considerably smaller than that attributed to viscous friction.

Thus, knowing the power applied to the mill shaft (from experiments or computations) we can determine the average particle oscillation velocity as $u_b = \sqrt{(8/\pi)\Theta}$ from Eq. 3.

Stress Analysis of a Particle Caught between Two Milling Beads

The forces acting on the particles caught between the beads during a bead–bead collision can be estimated. This collision is normally noncentral. We will limit our approximate analysis only to compression components of the forces (a shear component that is of the same order of magnitude as that of a compression component). Our estimations made using the developed model showed that velocities of the beads are relatively small (usually within $u_b < 1$ m/s). Then, assuming that the collisions are nearly elastic (we accepted this assumption for the hydrodynamic model), we may use the Hertz theory for elastic impact as a reasonable estimate.

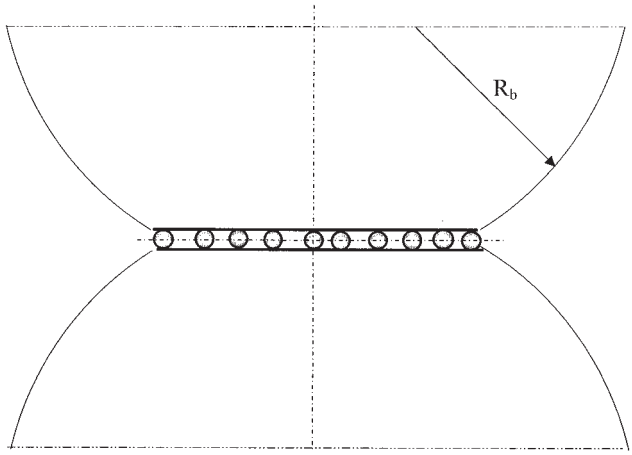

Figure 1. Bead–bead interaction.

Because we assumed that the distribution of beads velocities is Maxwellian, the probability density function for bead relative velocities is[20]

$$\omega(u_{brel}) = \left(\frac{1}{4\pi\Theta}\right)^{3/2}\exp\left(-\frac{u_{brel}^2}{4\Theta}\right)4\pi u_{brel}^2 \tag{13}$$

where u_{brel} is the relative bead–bead velocity. The mean relative bead–bead velocity is $\tilde{u}_b^{rel} = u_b\sqrt{2}$.

As a result of multiple bead–bead collisions, particles caught between the beads experience contact fatigue damage that leads to particle fracture. Mechanisms of fracture at the submicron scale under cyclic loading conditions are not well understood; therefore we restrict our attention to the simple analysis of the bead–bead and particle–bead contact interactions.

Let us consider the particle volumetric concentration to be $<10\%$. In this case we assume that only one layer of particles can be caught between the beads (Figure 1). Because of relatively low particle concentration and very significant size difference between the beads and nanoparticles, we assume that particles do not affect the interaction between beads (in terms of the contact stress, contact area, etc.). Then, we assume that the collision of two beads can be considered as the interaction between two elastic smooth spheres. The analysis below will show the validity of these assumptions. If the contact between two beads is elastic and smooth, the relations between the size of the contact area, the distributions of the normal contact pressure, and the normal force can be estimated using the Hertzian theory. In the case of oblique collision the size of the contact zone and the normal stress distribution are determined by the normal component of the contact force.[21]

The average maximum normal force F_b^n during collision of two identical elastic beads is determined as follows[22]:

$$F_b^n = 0.76\left[\frac{Y_b}{5(1-\eta_b^2)}\right]^{2/5}(2\pi\rho_b)^{3/5}(u_{brel}^n)^{6/5}(R_b)^2$$
$$= 1.96\left[\frac{Y_b}{(1-\eta_b^2)}\right]^{2/5}(\rho_b)^{3/5}(R_b)^2(\Theta)^{3/5} \quad (14)$$

where Y_b is the Young modulus of the bead material, η_b is the Poisson ratio of the bead material, ρ_b is the bead density, R_b is the bead radius, and u_{brel}^n is the projection of the bead–bead relative velocity on the line connecting centers of the colliding beads (estimated by the flow model). The projection u_{brel}^n, averaged over all possible beads mutual orientations, is calculated in the moving coordinate system (see, for example, Babukha and Shreiber[15]). The simple integration results in

$$u_{brel}^n = \frac{2}{3}u_{brel} = \frac{8}{3}\sqrt{\frac{\Theta}{\pi}} \quad (15)$$

The radius of the contact area between two beads α_b can be calculated as[22]

$$\alpha_b = \left[\frac{3}{4}\frac{(1-\eta_b^2)}{Y_b}R_bF_b^n\right]^{1/3} \quad (16)$$

The maximum contact pressure $\sigma_b^{\max}$ in the center of the contact area is

$$\sigma_b^{\max} = \frac{3}{2}\frac{F_b^n}{\pi(\alpha_b)^2} \quad (17)$$

The maximum approach between the beads in the normal direction is

$$\delta_b^n = 2\frac{(\alpha_b)^2}{R_b} \quad (18)$$

We examined several different types of bead material (steel, zirconia, polystyrene). The analysis shows that the contact between the beads under given relative bead velocity and the normal applied force (Eq. 14) is elastic, and the deformation is small and within Hooke's law, for all the media considered. To validate the assumption that the particles caught between the beads do not affect the size of the contact area as well as the normal stress distribution, we use the following arguments. First, because the initial size difference between the beads and the particles is about 2 to 3 orders of magnitude, we can approximately consider the bead–bead contact as that of a smooth bead with a rough bead coated with the particle layer, which can play the role of asperities. It was shown by Greenwood and Tripp[23] that, under high load, both the normal stress distribution and the size of the contact area at the elastic contact between the rough and smooth surfaces are not significantly different from the case of the elastic contact of two smooth surfaces. In spite of the presence of particles, the size of the contact area, as well as the maximum contact normal pressure in the beads, can be approximately determined from the solution for two smooth contacting spheres. In the case of the beads manufactured from soft material (such as polystyrene), the contact area (Eq. 16) is larger than that for hard beads (such as those made of zirconia). However, at the same time the maximum contact stress (Eq. 17) for the soft beads is much smaller than that for the hard beads. Thus, the hard media should be more efficient for grinding hard (hardly grindable) materials than soft ones. In the case of soft (easily grindable) materials the relatively low stresses developed in the particles may be sufficient to accumulate structural defects. The larger the contact zone, the greater the number of particles caught between the beads. Therefore, in the case of easily grindable particles the soft beads provide larger contact zones and may be more efficient than the hard media. We also analyzed how bead size influences the collision dynamics. The model of the slurry microhydrodynamics shows that larger beads have higher velocities. They provide larger contact zones and higher maximum normal contact pressures, although the frequency of their collisions is lower than that of smaller beads.

Increases in both contact area size and contact pressure expedite particle fatigue, whereas a decrease in collisional frequency decreases the grinding rate. The contributions of these concurrent processes to the grinding rate are different.

A simple model of particle fragmentation that we present below enabled us to estimate the grinding efficiency with respect to the bead size, bead density, and other mechanical parameters of milling media and solids.

Knowing the size of contact area, we may estimate the number of particles caught between two beads and the load applied to each individual particle. Estimates of the stresses in particles is much more complicated and depends on the type of particle deformation and history of loading. Multiple compressions cause nucleation of permanent structural defects that lead to crack initiation; the growth of cracks eventually results in particle fracture. Mechanisms of crack initiation can be different, depending on the material properties.[24]

Probability of Particle Stressing

For engineering estimates we neglect the polydispersity of particles that may influence the probability with which a particle can be caught between two beads (obviously larger particles are caught with higher probability). This simplification enables us to obtain the simple correlations that characterize basic regularities for this complicated multiparticle system.

The probability of a single particle being caught is estimated as the ratio of the volume containing the caught particles to the volume of solids–liquid suspension falling on a pair of the milling beads

$$p = \frac{2R_p\pi(\alpha_b)^2}{2\frac{4}{3}\pi(R_b)^3\frac{1-c}{c}}$$
$$= \frac{3}{4}\frac{c}{1-c}\frac{(0.57)^{2/3}}{(5)^{4/15}}\left[\frac{2\pi\rho_b(1-\eta_b^2)}{Y_b}\right]^{2/5}(u_{brel}^n)^{4/5}\frac{R_p}{R_b}$$
$$= 0.97\frac{c}{1-c}\left[\frac{\rho_b(1-\eta_b^2)}{Y_b}\right]^{2/5}(\Theta)^{2/5}\frac{R_p}{R_b} \quad (19)$$

The frequency of single-bead oscillations can be calculated by the following equation for Maxwellian gas[20]:

$$\nu = \frac{12cg_0}{R_b}\sqrt{\frac{\Theta}{\pi}} \tag{20}$$

The average number of particle compressions per unit time (frequency) can be estimated by assuming that these cyclic compressions can be considered as a Poisson process because it is characterized by small probability p and a high number of trials ν (see, for example, Bronstein and Semendyaev[25]). Then the mathematical expectation of this Poisson process equals the average frequency of particle compressions that is calculated as

$$\begin{aligned} a &= \nu p \\ &= \frac{(0.57)^{2/3}}{(5)^{4/15}}\frac{9c^2(2-c)}{2(1-c)^4}\left[\frac{2\pi\rho_b(1-\eta_b^2)}{Y_b}\right]^{2/5}(u^n_{brel})^{4/5}\frac{R_p}{(R_b)^2}\sqrt{\frac{\Theta}{\pi}} \\ &= 5.82\,\frac{1}{\sqrt{\pi}}\frac{c^2(2-c)}{(1-c)^4}\left[\frac{\rho_b(1-\eta_b^2)}{Y_b}\right]^{2/5}(\Theta)^{9/10}\frac{R_p}{(R_b)^2} \end{aligned} \tag{21}$$

A Simple Approach to Estimating the Grinding Efficiency

Because the particle fragmentation in a stirred media mill occurs as a result of multiple particle compressions, the grinding mechanism is associated with accumulation of structural defects in cyclically laden particles. Let us make estimations based on the energetic approach to simulation of batch grinding (for example, Charles[26]). For approximate analysis of the process consider an average particle size Z. Then instead of the particle radius R_p we will use the variable Z.

It is known that for many kinds of mills the equation relating the specific energy spent on grinding to the average particle size can be used[26]

$$dE = -\Omega\frac{dZ}{Z^\beta} \tag{22}$$

where E is the grinding energy per unit volume of material to be ground; Ω and β are empirical coefficients.

Let us determine the elementary specific energy dE as the work per unit volume done by external forces acting on the particle during the time dt. We consider the case of the normal elastic contact of the bead and the particle, and thus the elementary specific energy is

$$dE = \frac{aF^n_p s^n_p}{V_p}(1-c)\varepsilon dt \tag{23}$$

where F^n_p is the maximum average normal contact force between the particle and the bead, ζ^n_p is the particle normal displacement, and V_p is the particle volume.

Before calculating the particle deformation let us briefly discuss the change in the mechanical properties of the particles with decreasing particle size. It is well known that materials may display strong size effects when the characteristic length scale changes. Elastic response is basically independent of scale, down to atomistic scale, whereas in the case of plastic deformation there are at least five different length scales[27]: (1) atomistic (characteristic length is of the order of 0.1 nm), (2) discrete dislocations (characteristic length is of the order of 10 nm), (3) subgrain dislocation substructures (characteristic length is of the order of 100 nm), (4) grain (characteristic length is of the order of 10 μm), and (5) macroscale (characteristic length is of the order of 1 mm). On different length scales different plasticity theories should be applied. For example, conventional macroscopic theory of plasticity is valid on the macroscale,[28] whereas on the scale of subgrain dislocation substructures or mesoscale (such as 1–10 μm) the strain-gradient plasticity, which encompasses size effects, should be considered.[29,30] On the scale of discrete dislocations (such as 10–100 nm) the dislocation theory of plasticity is applied.[31]

Thus, scale effects assume substantial importance in the modeling of nanogrinding.

Note that on the scale of discrete dislocations the basic structure of conventional plasticity is preserved. Therefore for determination of submicron-particle deformation we use a simplified elastic–perfectly plastic model[28] with the yield strength that approaches the theoretical yield strength. This assumption is justified as follows. The experimental yield strengths of engineering materials are several orders of magnitude lower than the theoretical strengths (see, for example, Hertzberg[32]) because of the presence of thousands of dislocations. As the scale decreases to submicron range, the actual yield strength increases because the number of dislocations decreases and their movement becomes more discrete. Therefore, in our calculations of the deformation of submicron particles we suppose that the yield strength is one order of magnitude lower than the theoretical strength.[32]

For simplicity, we assume that the particle deformation is elastic–perfectly plastic and the deformation of the beads is elastic during the contact with particles. Additionally, we suppose that the fully plastic condition in the contact zone on the surface of the particles is reached, and the contact pressure σ_Y is constant across the contact zone. Let us denote by $F^n_{p,Y}$ the load when the first yield inside the particle occurs[22]

$$F^n_{p,Y} = \frac{\pi^3 R^{*2}}{6Y^{*2}}(\sigma_{0,Y})^3 \tag{24}$$

where

$$\frac{1}{R^*} = \frac{1}{R_b} + \frac{1}{R_p} \tag{25}$$

and

$$\frac{1}{Y^*} = \frac{1-\eta_b^2}{Y_b} + \frac{1-\eta_p^2}{Y_p} \tag{26}$$

Here η_p and Y_p are the particle's Poisson ratio and Young modulus, respectively, and $\sigma_{0,Y}$ is the maximum contact pressure at the first yield.

The normal force acting on the individual particle can be expressed as

$$F^n_p = \frac{F^n_b}{N_p} \tag{27}$$

where the number of particles N_p in the particle layer between two beads is determined as

$$N_p = \frac{\pi(\alpha_b)^2 2R_p}{V_p}\,\varepsilon \tag{28}$$

When the ratio $F_p^n/F_{p,Y}^n$ exceeds the certain critical value (at macroscopic scale $F_p^n/F_{p,Y}^n > 650$; see, for example, Johnson[22]), the particle contact zone is in the fully plastic condition. Thus, the normal force acting on the particle is

$$F_p^n = \pi(\alpha_p)^2\sigma_Y \tag{29}$$

Taking into account that $R_p \ll R_b$, we derive the particle normal displacement as

$$\varsigma_p^n \approx \frac{(\alpha_p)^2}{2R_p}\left(\frac{Y^*}{Y_p}\right)^{\gamma} \tag{30}$$

where $\gamma < 1$ is some coefficient ($\gamma = 1/3$ in the case of the elastic contact between the particle and the bead). In the case of the contact of a perfectly plastic particle with a rigid nondeformable bead, the normal displacement of the particle is

$$\varsigma_p^n = \frac{(\alpha_p)^2}{2R_p} \tag{31}$$

In a conventional theory, according to Johnson,[22] the fully plastic condition in the contact zone on the surface of a particle is reached when the contact pressure σ_Y is

$$\sigma_Y = 3\Sigma_Y \tag{32}$$

where Σ_Y is the yield stress of the material.

Taking into account Eqs. 27–30, 14–16, and 21 we represent the equation for the elementary specific (per unit volume) energy of particle deformation (Eq. 23) as

$$\begin{aligned} dE &= \frac{(2)^{38/5}(0.19)^{4/3}}{(3)^{19/15}(5)^{8/15}}\,\frac{c^2(2-c)}{(1-c)^3}\,\frac{1}{(\pi)^{5/2}\varepsilon\sigma_Y} \\ &\quad\times\left[\frac{Y_b}{(1-\eta_b^2)}\right]^{18/15}\left(\frac{Y^*}{Y_p}\right)^{\gamma}(\rho_b)^{4/5}\,\frac{R_p}{(R_b)^2}\,(\Theta)^{13/10}dt \\ &= 2.23\,\frac{c^2(2-c)}{(1-c)^3}\,\frac{1}{(\pi)^{5/2}\varepsilon\sigma_Y} \\ &\quad\times\left[\frac{Y_b}{(1-\eta_b^2)}\right]^{18/15}\left(\frac{Y^*}{Y_p}\right)^{\gamma}(\rho_b)^{4/5}\,\frac{R_p}{(R_b)^2}\,(\Theta)^{13/10}dt \end{aligned} \tag{33}$$

Thus

$$dE = \Psi(\Theta)^{13/10}Zdt \tag{34}$$

where

$$\begin{aligned} \Psi &= \frac{(2)^{38/5}(0.19)^{4/3}}{(3)^{19/15}(5)^{8/15}}\,\frac{c^2(2-c)}{(1-c)^3}\,\frac{1}{(\pi)^{5/2}\varepsilon\sigma_Y} \\ &\quad\times\left[\frac{Y_b}{(1-\eta_b^2)}\right]^{18/15}\left(\frac{Y^*}{Y_p}\right)^{\gamma}(\rho_b)^{4/5}\,\frac{1}{(R_b)^2} = 2.23 \\ &\times\frac{c^2(2-c)}{(1-c)^3}\,\frac{1}{(\pi)^{5/2}\varepsilon\sigma_Y}\left[\frac{Y_b}{(1-\eta_b^2)}\right]^{18/15}\left(\frac{Y^*}{Y_p}\right)^{\gamma}(\rho_b)^{4/5}\,\frac{1}{(R_b)^2} \end{aligned} \tag{35}$$

By integrating Eq. 22, and taking Eq. 35 into account, we obtain the following equation of the mean particle size reduction

$$Z = \left(\frac{1}{\frac{\beta\Psi}{\Omega}\,\Theta^{13/10}T + \frac{1}{Z_0^{\beta}}}\right)^{1/\beta} \tag{36}$$

where Z_0 is initial particle size at the initial moment of time T_0.

Thus, for predicting the change of the mean particle size in time we need to identify only two parameters from an experiment: Ω and β. The first approximation for the coefficient β follows from Rittinger's law of fine grinding[26]: $\beta = 2$.

Note, it is very important that the energy dissipation rate (dE/dt), resulting from solids deformation per unit volume, characterizes the grinding intensity and can be used as a criterion of grinding efficiency. The equation of the rate dE/dt explicitly follows from Eq. 33

$$\Pi = \frac{dE}{dt} = \Xi\Theta^{13/10} \tag{37}$$

The criterion Π may be used for analysis of a mill performance but it is not always sufficient to provide an unambiguous conclusion about the milling efficiency. The developed model of particle fragmentation is very simple. It does not take into account the real mechanism of generation of particle structural defects and change of particle mechanical properties ascribed to surfactants, which are necessary for nanogrinding. Moreover, the properties of nanoparticles are usually unknown. Thus, the model developed is suitable for qualitative analysis only. However, as one can see below (see Numerical Analysis and Discussions), this simple model predicts the basic trends of grinding and their dependency on the major process parameters.

Note that the criterion Π has the structure that is slightly similar to Eq. 12 for the dissipation energy rate ε_{coll} caused by partially inelastic bead–bead collisions. This is expected because the dissipation energy rate arising from solids deformation is a fraction of the energy dissipation rate ε_{coll}.

We also introduce a criterion that shows which part of the power on slurry stirring is spent on the energy dissipation arising from solids deformation

$$\eta = \frac{\Pi}{P_w} \tag{38}$$

This criterion may be useful for designing equipment of industrial scale because it characterizes the total energy expense on grinding.

Estimations of Power Spent on Slurry Agitation in a Regime of Developed Turbulence

It is now to possible to make an analysis that is useful for the scaling of stirred media mills. It is known that at large Reynolds numbers the energy per unit volume spent on turbulent mixing does not depend on the liquid (slurry) viscosity and is estimated as[7]

$$P_w = \varepsilon_{tot} \sim \rho_m \frac{U^3}{L} \tag{39}$$

where $\rho_m = \rho_b c + \rho_L(1 - c)$ is the slurry density, L is the characteristic size, and U is the characteristic velocity. For a stirred media mill the circumferential velocity of the stirrer can be chosen as a characteristic velocity and its radius as the characteristic size.

According to the theory of energy dissipation on the microscale, the bead oscillation velocities depend mainly on the energy dissipation rate, the media volumetric concentration, the bead size, and the bead density. Then, to substitute the certain milling media by others of the same size but at higher density—at the same time maintaining the same energy dissipation rate—the stirring velocity U should be decreased in accordance with Eq. 39. As a result the beads' oscillation velocities will be the same. However, Eq. 14 shows that at the same oscillation velocities heavier beads cause greater forces at the bead–bead interactions.

Numerical Analysis and Discussions

It is a complicated problem to calculate power consumed by a stirred media mill because there are many different types of stirrers. It follows from the approach developed here that the mill performance depends to a great extent on the energy dissipation rate. From this perspective, if we provide the same energy dissipation rate at the same milling medium by different stirrers the mean bead oscillation velocity will be the same and in turn should lead to the same grinding rate; this is true if it is assumed that the energy dissipation rate is uniformly distributed over the milling chamber. In practice this distribution may be nonuniform and depends on the stirrer design; therefore only experiments with various stirrers and the same energy dissipation rate may provide a conclusive explanation as to how stirrers affect the grinding efficiency.

To make a simple illustrative analysis, instead of mixing in a stirred media mill, we will consider the well-studied stirring process in a mixing tank, where Rushton-type paddles perform the agitation. The specific power of agitation in mixing tanks of many designs is calculated as[10]

$$P_w = M\rho_m \frac{N^3 D^5}{\Lambda^2 H} \tag{40}$$

where D is the stirrer diameter, H is the height of a mixing tank, M is the coefficient, N is the stirrer rotation speed, and Λ is the mixing tank diameter.

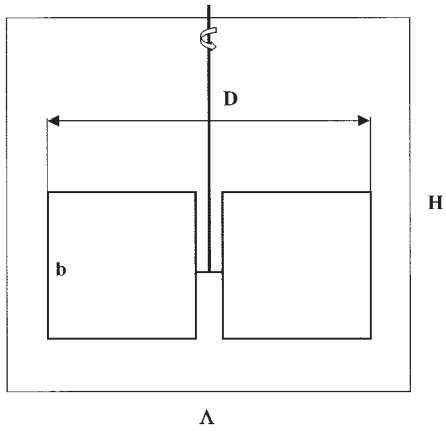

Figure 2. Schematic of the slurry mixer.

For our estimates we chose a mixing tank (Figure 2) of diameter $\Lambda = 0.1$ m, height $H = 0.16$ m, equipped with the stirrer of diameter $D = 0.8\Lambda$. This stirrer has one paddle (two blades) of width $b = 0.5D$. The coefficient M is determined by the empirical correlation for a single paddle

$$M = \frac{A}{\mathrm{Re}} + B\left(\frac{10^3 + 1.2\,\mathrm{Re}^{0.66}}{10^3 + 3.2\,\mathrm{Re}^{0.66}}\right)^h \tag{41}$$

where $\mathrm{Re} = D^2 N\rho_m/\mu_m$, g is the gravitational acceleration, and

$$A = 14 + \frac{b}{\Lambda}\left[670\left(\frac{D}{\Lambda} - 0.6\right)^2 + 185\right]$$

$$B = 10^{[1.3 - 4(b/\Lambda - 0.5)^2 - 1.14(D/\Lambda)]}$$

$$h = 1.1 + 4\frac{b}{\Lambda} - 2.5\left(\frac{D}{\Lambda} - 0.5\right)^2 - 7\left(\frac{b}{\Lambda}\right)^4$$

The slurry dynamic viscosity can be calculated by the following empirical correlation[33]

$$\mu_m = \mu_L[1 + 2.5c + 10c^2 + 0.0019\exp(20c)] \tag{42}$$

Figure 3 shows the average bead oscillation velocities against the rotation speed at different bead sizes (d_b values of 50 and 200 μm) and densities [ρ_b values of 1000 (polystyrene) and 7800 kg/m^3 (steel)]. The velocities increase almost linearly with increasing rotation speed. The steel beads have higher oscillation velocities than those of polystyrene beads of the same size. This is explained by the higher energy dissipation rate on mixing the slurry consisting of the heavier (steel) beads because the power on stirring linearly increases with increasing slurry density (Eq. 39).

In Figure 4 one can see the dependency of the number of particles compressed between the beads on the bead size for the steel and polystyrene media, respectively. These calculations were carried out for nanoparticles of size $d_p = 20$ nm, solids volumetric concentration $\varepsilon = 0.075$, volumetric concentration of beads $c = 0.4$, and stirrer rotation speed $N = 9000$ rpm. The number of particles caught rapidly decreases with decreasing

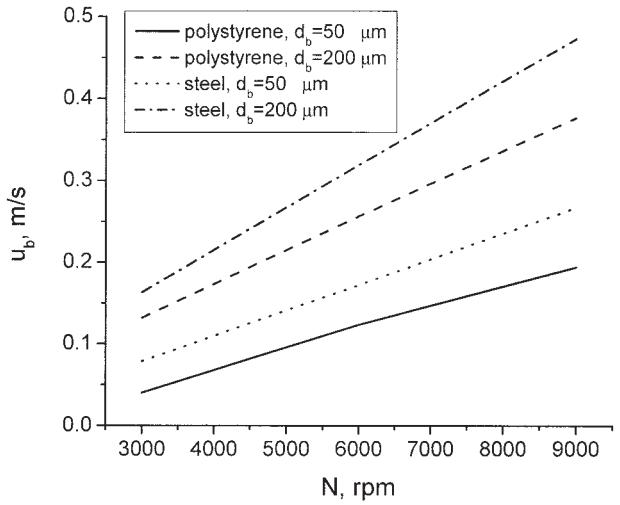

Figure 3. Average oscillation velocities of the different media against the stirrer rotation speed.

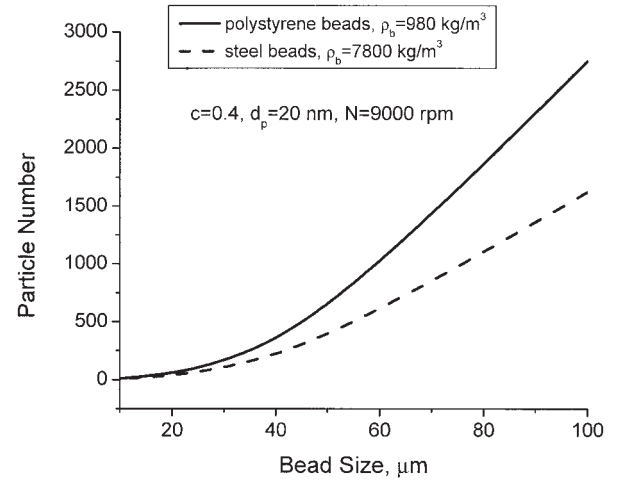

Figure 4. Dependency of the number of particles compressed between the beads on the bead size for the steel and polystyrene media.

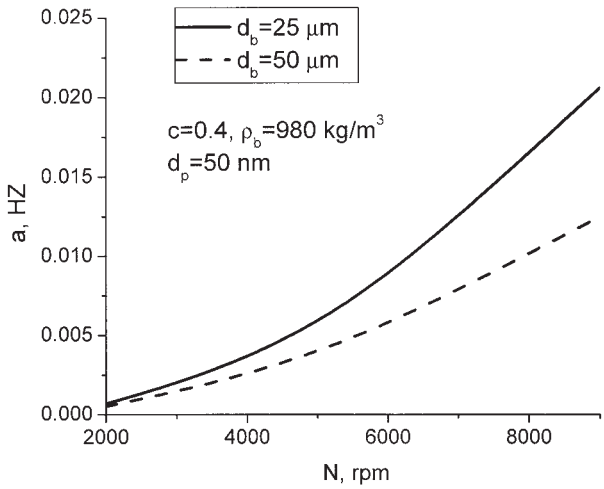

Figure 5. Frequencies of particle compressions between the polystyrene beads of two different sizes vs. the stirrer rotation speed.

bead size. It is important to emphasize that this number is not significantly lower for the case of the steel beads, although they have much higher elasticity modulus. Because of the high inertia the stiff steel beads deform similarly to the soft polystyrene beads.

Below, we present a number of computational examples for polystyrene milling media. This is because the polystyrene beads showed good performance at nanogrinding of some materials (an organic pigment was ground to the median size of 10 nm). One of the plausible hypotheses explaining this phenomenon is that the particles are embedded in the relatively soft surface of the milling beads and then this surface, coated by particles, becomes as hard as the ground material, which leads to the grinding intensification. This effect is a kind of autogenous grinding. However, this hypothesis has not yet been proven experimentally. Note that another problem of experimental research is the difficulty of measuring the mechanical properties of nanosize particles. The mechanical properties of the polystyrene considered are: the Young modulus of the polystyrene considered is $Y_b = 3.8$ GPa and the Poisson ratio is $\nu_b = 0.4$.

The particle size and the particle density were kept the same for all computational examples presented below: $d_p = 50$ nm and $\varepsilon = 0.075$, respectively. The mechanical properties of the material were selected as follows. The particle Young modulus and Poisson ratio were equal to those of milling beads, and the particle material yield stress was $\Sigma_y = 0.38$ GPa that is one order of magnitude lower than the particle Young modulus, as might be expected for nanoparticles (see A Simple Approach to Estimating the Grinding Efficiency).

In Figure 5 we show the frequencies of particle compressions between the polystyrene beads of two different sizes (d_b values of 25 and 50 μm) vs. the stirrer rotation speed. The frequencies increase with increasing rotation speed and they are significantly higher for the smaller beads, which is explained by the fact that the media numerical concentration is inversely proportional to the third power of the size of the beads.

In Figure 6 one can see the frequency of particle compressions vs. the bead concentration for the beads of size $d_b = 25$ μm. The calculations were performed for rotational speeds N of 4000 and 9000 rpm. The frequency increases with increasing concentration, which follows from Eq. 21.

In Figure 7 we plotted the criterion Π (see Eqs. 33–37) vs. the bead size for three different rotation speeds (N): 4000, 6000, and 9000 rpm, respectively. One can see that there are bead sizes that provide the maximum of Π at each rotation speed. The optimum bead size decreases with increasing rotation speed. Note that this extremum becomes sharper with increasing speed N, whereas at the relatively low rotation speed ($N = 4000$ rpm) the maximum milling efficiency is almost constant in the wide range of media sizes. On the one hand, the criterion rapidly increases with increasing granular temperature, which increases with increasing rotation speed. On the other hand, the granular temperature decreases with decreasing bead size. The relative contribution of both these factors to the

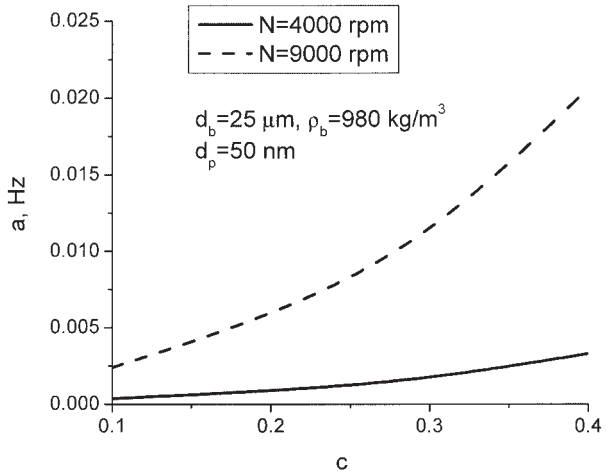

Figure 6. Frequency of particle compressions vs. the bead concentration for beads of size d_b = 25 μm.

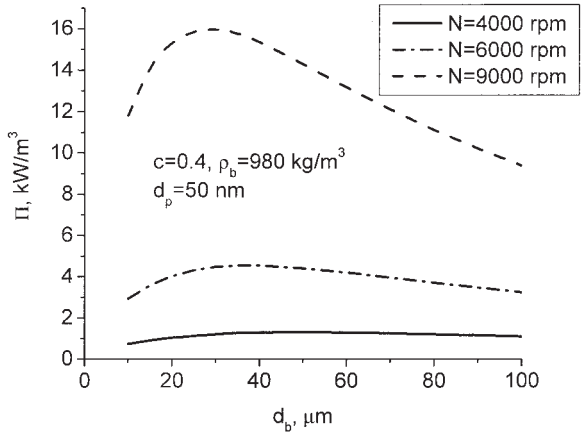

Figure 7. Solids energy deformation rate per unit volume vs. the bead size for three different stirrer rotation speeds.

granular temperature change determines the behavior of the criterion Π.

In Figure 8 we show the change of the median particle size during the grinding of an organic pigment in the laboratory mill with a volume 0.5 L. The pigment was ground to nanosizes by using three sets of polystyrene beads of sizes (d_b) of 10, 25, and 50 μm, respectively. One can see that the 20- and 50-μm media provide almost the same grinding rate. The 10-μm beads do not provide visible changes of the median particle diameter because the stresses developed in particles in this case are not sufficient to cause particle fragmentation. These results agree with our grinding theory because one can see in Figure 7 that at the small rotation speed (N = 4000 rpm) the criterion Π almost does not change in the media size range d_b = 25–100 μm, whereas it significantly decreases when the media sizes are smaller than d_b = 20 μm. Note that the stirrer rotation speed in the experiments was only 2000 rpm. Although the data on power expenses for stirrer rotation were not available, it is clear that the power required for stirring in the mill is higher than that in the calculated mixer at the same rotation speed.

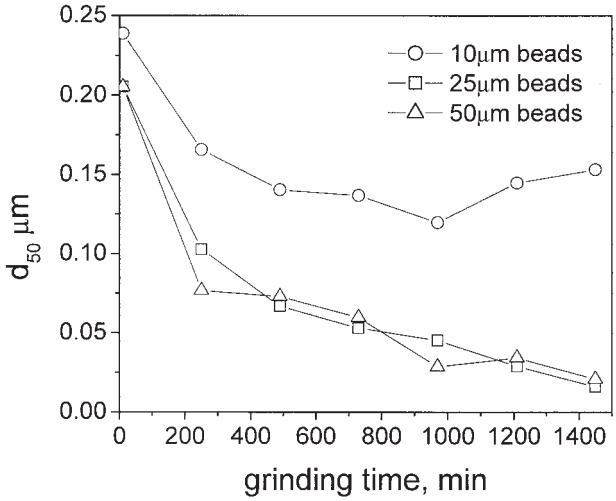

Figure 8. Change of the median particle size during grinding of the organic pigment in the laboratory mill, using three different milling media sizes.

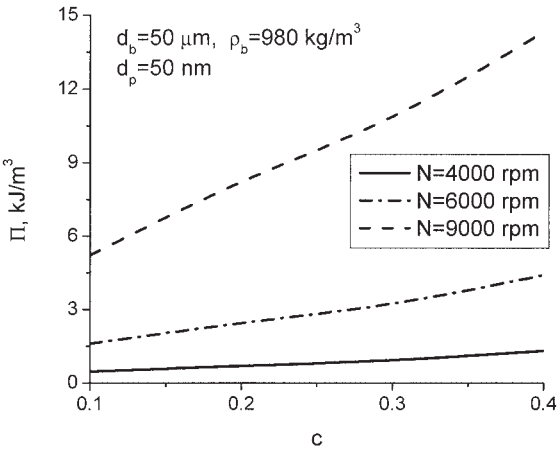

Figure 9. Solids energy deformation rate per unit volume vs. the media volumetric concentration at three different rotation speeds.

This is because the mill stirrer consists of six equally spaced vertical columns with the small clearance (3 mm) between the columns and the vessel wall. Because the energy dissipation in the mill corresponds to the larger rotation speed calculated in the mixer, we computed the mixers with the minimum rotation speed N = 4000 rpm. Note that macrohydrodynamics of stirring in the mill supplied with the six-column stirrer is very different from that having the paddle stirrer and thus these estimations are fairly approximate. In industrial applications the power can accurately be determined through measuring the torque applied to the stirrer.

In Figure 9 we show the criterion Π vs. the media volumetric concentration at different rotation speeds. The particle deformation energy rapidly increases with increasing concentration of the beads, in an almost linearly dependent manner. This behavior of the criterion Π is observed because increasing the media concentration leads to a more significant increase in the

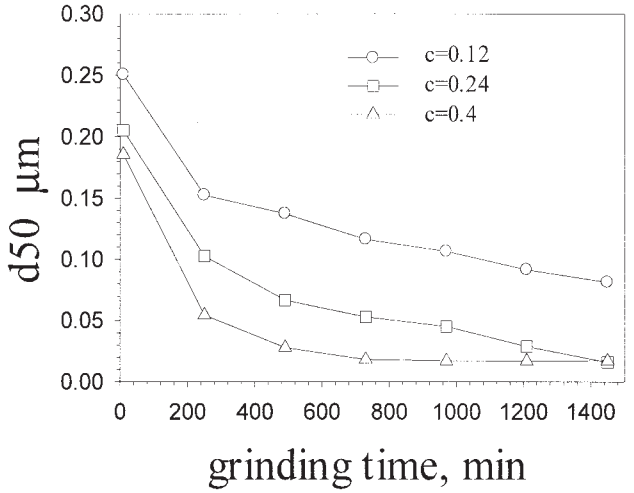

Figure 10. Change of the median particle size in time at grinding of the organic pigment in the laboratory mill at three different milling media concentrations.

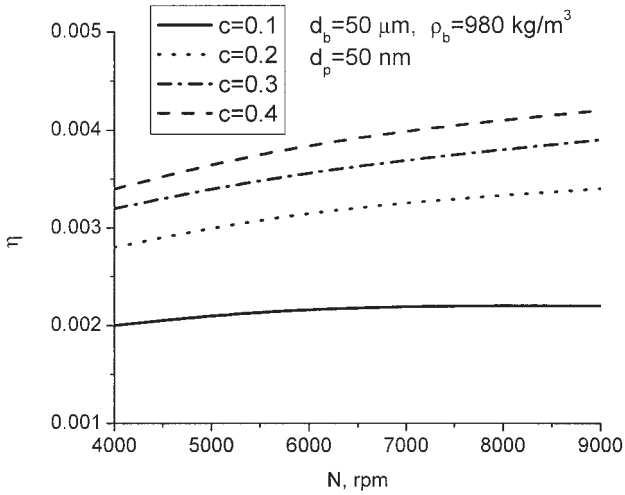

Figure 11. Criterion of grinding efficiency against the stirrer rotation speed.

frequency of bead–bead collisions than the corresponding decrease in the media granular temperature (see Eq. 20). These theoretical results are confirmed by the experimental data. In Figure 10 we show the change of the median particle size in time of grinding for the same pigment in the same experimental mill for the three different milling media concentrations (c values of 0.12, 0.24, and 0.4). The media size was $d_b = 50$ μm and the stirrer rotation speed was $N = 2000$ rpm. One can see that the higher the media concentration, the higher the grinding rate.

To demonstrate that only a very small fraction of energy spent on stirring is transformed into the deformation of particles, in Figure 11 we show the calculated efficiency criterion η against the stirrer rotation speed. The milling media size was $d_b = 50$ μm. This figure reflects the tendencies made clear from Figures 7–10, although the values of the criterion η show that only a fraction of a percentage of the energy spent on slurry stirring is transformed into the energy of particle deformation. In turn, the energy spent on fracture of molecular bonds is a small fraction of the energy of the particle deformation, which thus confirms that nanogrinding is a very energy consuming process.

Thus, the analysis of flow hydrodynamics in a stirred media mill showed that, to provide the maximum total energy of particle deformation, it is necessary to choose the optimum bead size, high bead concentration, and the rotation speed, respectively. However, the choice of these parameters depends, to a greater extent, on mechanical properties of solids to be ground. It is clear that easily grindable materials do not require the highest rotation speed. Note also that the increase in media concentration is reasonable only to the level at which the flow turbulent regime is maintained.

Thus, the most important results of our microhydrodynamic analysis are as follows. We developed the method that enables us to estimate the relative velocities of the colliding beads, and the frequency of particle compressions caught between the beads. A supposition about the plastic deformation of nanoparticles allowed us to predict the optimum bead size that qualitatively agreed with the experiment. Thus, we proposed an approach to modeling the dynamics of milling media and solid particles in stirred media mills that is an important step for optimization and scaling-up of equipment.

Conclusions

Dynamics of the milling beads in a turbulent flow has been considered. The beads' mean velocities were calculated on the basis of the hypothesis that the power spent on stirring is transferred into the energy of turbulent eddies that dissipates as a result of bead–liquid viscous friction, lubrication, and partially inelastic collisions of the beads with each other. The maximum force, with which milling beads compress particles between them, was estimated by the Hertzian theory of elastic impact. The frequency of compressions for a single particle was evaluated by probabilistic analysis. The method of estimating the total energy spent on solids deformation was proposed. Numerical studies of the stirred media mill performance and dependency on different process parameters were performed. One of the most important results obtained was predicting the media size that provides the maximum total energy on solids deformation. The computational data were qualitatively confirmed by analysis of the experimental grinding rates with use of different media sizes. The computations also showed that increasing media concentration leads to increasing particle deformation energy rate. The experiments revealed that increasing grinding rate was caused by increasing bead concentration. Thus, the numerical analysis showed that the optimization of stirred media mills from the perspective of hydrodynamics should be reduced to calculating the optimum bead size and increasing the bead concentration to the maximum level obtainable.

Acknowledgments

The authors acknowledge the financial support of the Particle Engineering Research Center (PERC) at the University of Florida, the National Science Foundation (NSF) Grant EEC-94-0289, and the Industrial Partners of the PERC. Dr. D. Eskin thanks Dr. A. Vikhansky (Cambridge University) for useful discussions.

Notation

a = average frequency of particle compressions, Hz
b = mixer blade width, m
c = solids volumetric concentration
c_{lim} = theoretical limiting (packing) solids concentration
D = stirrer diameter, m
d_b = milling bead size, m
d_p = particle size, m
d_5 = median particle size, m
E = energy on grinding per unit volume of material, J/m^3
F = average drag force acting on a single bead, N
F_b = average maximum normal force during collision of two identical elastic beads, N
F_b^n = average maximum normal force during collision of two identical elastic beads, N
F_p^n = average normal force acting on the individual particle, N
F_c = average compressing force acting on interacting bubbles, N
g = radial distribution function
H = height of the mixing tank, m
k = restitution coefficient for bead–bead collisions
$K(c)$ = coefficient
L = characteristic stirrer size, m
n_b = media numerical concentration, 1/m^3
N = stirrer rotation speed, 1/s
N_p = number of particles caught between two beads
p = probability to be caught between the beads for a single particle
P_w = power applied to the stirrer per unit volume, W/m^3
Re = Reynolds number based on the stirrer tip velocity
Re_Θ = bead Reynolds number based on the granular temperature
R_{diss} = dissipation coefficient that can be interpreted as an effective drag coefficient of the bead
R_{diss} = dissipation coefficient taking into account squeezing the liquid film
R = radius, m
T = grinding time, s
u_b = average particle oscillation velocity, m/s
u_{brel} = relative bead–bead velocity, m/s
$\tilde{u}_b^{rel}$ = mean relative bead–bead velocity, m/s
U = characteristic velocity, m/s
Y = Young modulus of the beads, Pa
V_p = particle volume, m^3
W = ratio of the bead relaxation time to the mean time of the bead free motion between collisions
Z = particle size, m

Greek letters

α = radius of the contact area at the contact of two spheres, m
β = empirical coefficient
δ = average clearance between the beads in a slurry flow, m
ε_{coll} = energy dissipation rate arising from partially inelastic bead–bead collisions, W/m^3
ε_{tot} = total rate of energy dissipation, W/m^3
ε_{visc} = energy dissipation rate attributed to both the liquid–beads viscous friction and lubrication, W/m^3
ε_m = nondimensional particle–particle gap thickness at which the lubrication force stops continuous increase and becomes a constant
η = part of the energy spent on slurry stirring transforms into the energy of particle deformation
η_b = Poisson modulus of the bead material
η_p = Poisson modulus of the particle material
λ = inner turbulence scale, m
Λ = mixing tank diameter, m
μ = dynamic viscosity, kg/ms
ν = frequency of single-bead oscillations, 1/s
ν_m = slurry kinematic viscosity, m^2/s
Π = dissipation energy rate attributed to solids deformation per unit volume, W/m^3
Θ = granular temperature, m^2/s^2
ρ = density, kg/m^3
σ_b^{max} = maximum contact pressure in the center of the contact area, Pa
σ_y = contact pressure in particle when the fully plastic condition is obtained, Pa
$\sigma_{0,Y}$ = maximum contact pressure at the first yield, Pa
$\omega(u_{brel})$ = probability density function for bead relative velocities, s/m
Ω = empirical coefficient, J/m$^{4-\beta}$
$\langle v_b \rangle$ = bead–liquid relative rms velocity, m/s
ζ = normal displacement of a compressed sphere, m

Indices

b = beads
c = collisional
L = liquid
m = mixture
n = normal
p = particles
rel = relative
tot = total
y = yield
$visc$ = viscous
Θ = related to granular temperature
5 = median

Literature Cited

1. Kwade A. Wet comminution in stirred media mills—Research and its practical application. *Powder Technol.* 1999;105:14-20.
2. Kwade A, Schwedes J. Breaking characteristics of different materials and their effect on stress intensity and stress number in stirred media mills. *Powder Technol.* 2002;122:109-121.
3. Jankovic A. Variables affecting the fine grinding of minerals using stirred mills. *Miner Eng.* 2003;16:337-345.
4. Blecher L, Kwade A, Schwedes J. Motion and stree intensity of grinding beads in a stirred media mill. *Powder Technol.* 1995;86:59-68.
5. Theuerkauf J, Schwedes J. Theoretical and experimental investigation on motion in stirred media mills. *Powder Technol.* 1999;105:406-412.
6. Khodakov GS. Physicochemical mechanics of grinding of solids. *Colloid J.* 1998;60:631-643.
7. Landau LD, Lifshiz EM. *Fluid Mechanics*. London: Pergamon; 1959.
8. Levich VG. *Physicochemical Hydrodynamics*. Engelwood Cliffs, NJ: Prentice-Hall; 1962.
9. Schook CA, Roco MC. *Slurry Flow*. London: Butterworth-Heinemann; 1991.
10. Nagata S. *Mixing: Principles and Applications*. New York, NY: Wiley; 1975.
11. Wylie JJ, Koch DL, Ladd AJC. Rheology of suspensions with high particle inertia and moderate fluid inertia. *J Fluid Mech.* 2003;480:95-118.
12. Eskin D, Leonenko Y, Vinogradov O. On a turbulence model for slurry flow in pipelines. *Chem Eng Sci.* 2004;59:557-565.
13. Sangani AS, Mo GB, Tsao HK, Koch DL. Simple shear flows of dense gas–solid suspensions at finite Stokes numbers. *J Fluid Mech.* 1996;313:309-341.
14. Carnahan NF, Starling KE. Equation of state for nonattracting rigid spheres. *J Chem Phys.* 1969;51:635.
15. Babukha G, Shreiber A. *Interaction of Polydispersed Particles in Gas Flows* (in Russian). Kiev, Ukraine: Naukova Dumka; 1972.
16. Drazer G, Koplik J, Khusid B, Acrivos A. Deterministic and stochastic behavior of non-Brownian spheres in sheared suspensions. *J Fluid Mech.* 2002;460:307-335.
17. Marchioro M, Acrivos A. Shear-induced particle diffusivities from numerical simulations. *J Fluid Mech.* 2001;443:101-128.
18. Wylie JJ, Koch DL. Particle clustering due to hydrodynamics interactions. *Phys Fluids.* 2000;12:964-970.
19. Gidaspow D. *Multiphase Flow and Fluidization: Continuum and Kinetic Theory Descriptions*. Boston, MA: Academic Press; 1994.
20. Chapman S, Cowling TG. *The Mathematical Theory of Non-Uniform Gases*. Cambridge, UK: Cambridge Univ. Press; 1970.
21. Goldsmith W. *Impact: The Theory and Physical Behaviour of Colliding Solids*. London: Edward Arnold; 1960.
22. Johnson KL. *Contact Mechanics*. Cambridge, UK: Cambridge Univ. Press, 1985.

23. Greenwood JA, Tripp JH. The elastic contact of rough spheres. *ASME J Appl Mech.* 1967;34:153-159.
24. Suresh S. *Fatigue of Materials*. Cambridge, UK: Cambridge Univ. Press; 1998.
25. Bronstein IN, Semendyaev KA. *Mathematics Handbook*. Moscow: Nauka; 1986.
26. Charles RJ. Energy-size reduction relationships in comminution. *AIME Trans.* 1957;208:80-88.
27. McDowell DL. Modeling and experiments in plasticity. *Int J Solids Struct.* 2000;37:293-309.
28. Malvern LE. *Introduction to the Mechanics of a Continuous Medium*. Englewood Cliffs, NJ: Prentice-Hall; 1969.
29. Fleck NA, Hutchinson JW. A reformulation of strain gradient plasticity. *J Mech Phys Solids.* 2001;49:2245-2271.
30. Gao H, Huang Y, Nix WD, Hutchinson JW. Mechanism-based strain gradient plasticity—I. Theory. *J Mech Phys Solids.* 1999;47:1239-1263.
31. Khan AS, Huang S. *Continuum Theory of Plasticity*. New York, NY: Wiley; 1995.
32. Hertzberg RW. *Deformation and Fracture Mechanics of Engineering Materials*. New York, NY: Wiley; 1976.
33. Gillies R, Shook CA. Modeling high concentration settling slurry flows. *Can J Chem Eng.* 2000;75:709-716.

Manuscript received Jan. 9, 2004, and revision received Aug. 26, 2004.